

SYNTHESIS, CHARACTERIZATION AND BIOACTIVITY Zn²⁺, Cu²⁺, Ni²⁺, Co²⁺, Mn²⁺, Fe³⁺, Ru³⁺, VO²⁺ and UO₂²⁺ COMPLEXES OF 2-HYDROXY-5-((4-NITROPHENYL) DIAZENYL)BENZYLIDENE)-2-(*p*-TOLYLAMINO)ACETOHYDRAZIDE

Mohamad M.E. Shakdofa^{1,2*}, Ahmed N. Al-Hakimi^{3,4}, Fathy A. Elsaied⁵, Samir O.M. Alasbahi⁶ and Ashwaq M.A. Alkwlini⁵

¹Chemistry Department, Faculty of Sciences and Arts, Khulais, University of Jeddah, Saudi Arabia

²National Research Centre, Inorganic Chemistry Department, El-bohouh Street, Dokki, Cairo, Egypt

³Faculty of Science, Chemistry Department, Qassim University, Qassim, Saudi Arabia

⁴Faculty of Science, Chemistry Department, Ibb University, Ibb, Yemen

⁵Faculty of Science, Department of Chemistry, El-Menoufia University, Shebin El-Kom, Egypt

⁶Faculty of Science, Physics Department, Ibb University, Ibb, Yemen

(Received November 15, 2015; revised February 5, 2017)

ABSTRACT. Novel azo-acetohydrazide complexes of Zn²⁺, Cu²⁺, Ni²⁺, Co²⁺, Mn²⁺, Fe³⁺, Ru³⁺, VO²⁺ and UO₂²⁺ with 2-hydroxy-5-((4-nitrophenyl)diazenyl)benzylidene)-2-(*p*-tolylamino)acetohydrazide have been prepared. All the compounds were analytically and spectroscopically characterized by various techniques. The data of molar conductance indicated the prepared complexes are nonelectrolyte in nature except complexes (10) and (11). The spectroscopic data point out that the behavior of ligand towards metal ions are neutral or monobasic bidentate, and dibasic tridentate ligand linked to the metal ions through oxygen atom of ketonic or enolic carbonyl group, azomethine nitrogen atom and/or deprotonated phenolic group forming either octahedral or tetragonally distorted octahedral geometry. X-ray powder diffraction analysis of complexes (2) and (3) indicate that the complexes are crystalline in nature and have monoclinic structures. The microbicidic activities of all compounds evaluated by well diffusion method versus *Escherichia coli* and *Aspergillus niger* at different concentration. The bioactivities data elucidated that as the concentration of the tested solutions increases the activities increase.

KEY WORDS: Azo-acetohydrazide, Azo-hydrazone, Metal complexes, Bioactivity, X-ray diffraction analysis

INTRODUCTION

Hydrazine and hydrazone are a category of Schiff base which having N-N linkage. They have engaged significant interest to chemist and medical researchers for several decades, in order to their various biological and pharmaceutically implementations. hydrazone compounds and their transition metal complexes possess obvious biologically and pharmaceutically liveliness in medical chemistry, such as antimicrobial [1], antibacterial [2], antifungal [2], anticancer [3], antitumor [4], anticandidal [3], antitubercular [5], analgesic, anti-inflammatory [6], anticonvulsant [7], and leishmanicidal activities [8]. The derivatives N-2-(4-benzylpiperidin-piperazin-1-yl)acylhydrazone were tested in the treatment of Alzheimer diseases which have inhibition ability of acetylcholinesterase, butyryl cholinesterase and assemblage of amyloid beta peptides [9]. N-[(2,4-dihydroxyphenyl)methylidene]-2-(3,4-dimethyl-5,5-dioxidopyrazolo[4,3-c][1,2]benzothiazin-1-(4H)-yl)acetohydrazide have anti-arthritic activity [10]. Cu²⁺, Co²⁺ and Ni²⁺ complexes N-[1-(pyridin-2-yl)ethylidene] acetohydrazide thiocyanato-bridged zig-zag polymers have inhibition effects on the outgrowth of human carcinoma cells of lung, hepatocellular and colorectal [11]. Cu²⁺ and Zn²⁺ complexes of 2-(naphthalen-1-yloxy)-N-(1-(pyridin-2-yl)ethylidene)acetohydrazide revealed a considerable anti-inflammatory and analgesic effect [12]. 2-(Quinolin-8-yloxy)acetohydrazones and their cyclized 1,2,3-thiadiazole

*Corresponding author. E-mail: mshakdofa@gmail.com

and 1,2,3-selenadiazole derivatives have anti-amoebic activity against *Entamoeba histolytica* [13]. Hydrazone ligands serve as extracting agents in spectrophotometric estimation of some ions and species in pharmaceutical formulations [14] as long as its utilization in treatments of wastewater and catalytic processes [15]. Furthermore, azo compounds have an increased attention from researchers [16]. Metal complexes of azo compounds are recognized to be taken part in some biological reactions, like DNA, RNA inhibition, synthesis of protein, fixation of nitrogen, and carcinogenesis [17]. Moreover, the azo ligands and their complexes are highly utilized in data storage and dyes [18]. In view of these above multiple importance, we planned to synthesize novel azohydrazone ligand containing azo group as a side chain resulted from condensation of 2-hydroxy-5-((4-nitrophenyl)diazonyl)benzaldehyde with 2-(*p*-tolylamino)acetohydrazide. The work extended to synthesis the Zn^{2+} , Ni^{2+} , Cu^{2+} , Co^{2+} , Mn^{2+} , Ru^{3+} , Fe^{3+} , VO^{2+} and UO_2^{2+} complexes with the prepared ligand to evaluate the effect of azo group on the microbicidal activities of the prepared compounds. All compounds were characterized by spectroscopic and analytical tools like elemental and thermal, magnetic susceptibility, molar conductance measurements, spectral (UV-Visible, IR, 1H -, ^{13}C -NMR) and X-ray diffraction.

EXPERIMENTAL

Materials

All chemicals utilized in the ligand and metal complexes preparations were of analytical grade available and applied without extra purification. 2-(*p*-Tolylamino)acetohydrazide and 2-hydroxy-5-((4-nitrophenyl)diazonyl)benzaldehyde were synthesized by published methods [19, 20]. Dimethyl sulfoxide (assay 99.80 %) and absolute ethyl alcohol (assay \geq 99.90 %) were used. Metal salts were provided from Sigma-Aldrich Company (purity from 98% to 99.99%). TLC tool was used to confirm the pureness of all synthesized compounds.

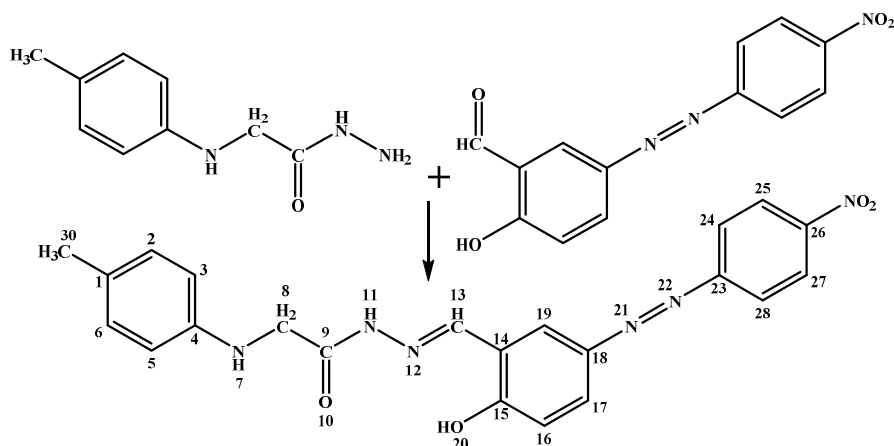
Instrumentation and measurements

The elemental analysis (CHN) was recorded in the Analytical Unit of Cairo University (Egypt). The metal ions content was estimated by standard analytical methods [21]. The ligand and metal complexes IR spectra were recorded on Perkin Elmer 1430 spectrometer as KBr pellets in the Analytical Unit of Cairo University, Egypt. The 1H - and ^{13}C -NMR spectra were recorded on a JEOL JNM-ECP-400 MHz FT-NMR spectrometer in $DMSO-d_6$, where the chemical shifts were determined relative to the solvent peaks. XRD were recorded on RIGAKU ULTIMA IV in King Saud University, Saudi Arabia. The molar conductance of 10^{-3} M concentration metal complexes in DMF was recorded by a dip cell and a Bibby conductometer MC1 at room temperature. Electronic absorption spectra were measured in DMF by UV-6100PCS double beam spectrometer using 1 cm quartz cell. The Gouy method were used to measure the magnetic susceptibilities at room temperature using mercuric tetrathiocyanatocobaltate(II) as the magnetic susceptibility standard. Diamagnetic corrections were computed using Pascal's constant [22]. Shimadzu DT-30 thermal analyzer was used to carry out thermal analysis in the air on from 27 to 800 °C with heating rate of 10 °C per minute.

Preparation of ligand, 2-hydroxy-5-((4-nitrophenyl)diazonyl)benzylidene)-2-(phenylamino)acetohydrazide (H_2L) (I)

The ethanolic solution of 2-hydroxy-5-((4-nitrophenyl)diazonyl)benzaldehyde [20] (271.2 mg, 1 mmol, in 20 mL of absolute ethanol) was refluxed while stirring for one hour with ethanolic solution of 2-(*p*-tolylamino)acetohydrazide (179.3 mg, 1 mmol, in 20 mL of absolute ethanol). The formed yellow precipitate was filtered off, washed with cold ethyl alcohol and crystallized

from ethyl alcohol and dehydrated under vacuum over anhydrous CaCl_2 . Ligand H_2L (**1**), $\text{C}_{22}\text{H}_{20}\text{N}_6\text{O}_4$ (FW = 432.43), yield: 78%, melting points (m.p.) > 240; color: yellow. Elemental anal. calcd.: C, 61.00; H, 4.66; N, 19.43. Found: C, 61.10; H, 4.60; N, 19.22. IR, (KBr, cm^{-1}): 3360(s) $\nu(\text{OH})$, $\nu(\text{NH}^{\text{I}})$, 3253, $\nu(\text{NH}^{\text{II}})$ 3130, 1692 $\nu(\text{C}=\text{O})$, 1613 $\nu(\text{C}=\text{N})$, 1477 $\nu(\text{N}=\text{N})$, 1265 $\nu(\text{C}-\text{O})_{\text{ph}}$, 954 $\nu(\text{N}-\text{N})$. $^1\text{H-NMR}$ (DMSO-d_6 , 400 MHz): δ = 11.5 (s, 1H, OH), 11.80 (s, 1H, NH^{I}), 5.80 (s, 1H, NH^{II}), 8.59 (s, 1H, $\text{N}=\text{C}-\text{H}^{\text{III}}$), 6.50-8.40 ppm (m, 11 H, aromatic protons). $^{13}\text{C-NMR}$ (DMSO-d_6 , 400 MHz): δ = 172 (C=O), 167.9 (C-OH), 161, 158 (C-N=N-C), 155.9 (C-NO₂), 148.5 (C-NH), 146.5 (C=NH), 113–135 (aromatic carbon), 41 (N-CH₂), 21.50 (CH₃).



Scheme 1. Preparation of ligand, 2-hydroxy-5-((4-nitrophenyl)diazenyl)benzylidene-2-(*p*-tolylamino)acetohydrazide.

Metal complexes preparation

Metal complexes, (**3-4**), (**7-8**) and (**10-13**) were synthesized by refluxing with stirring for 3 hours ethanolic solution of the following salts: $\text{CuCl}_2 \cdot 2\text{H}_2\text{O}$, $\text{CuSO}_4 \cdot 5\text{H}_2\text{O}$, $\text{Co}(\text{CH}_3\text{COO})_2 \cdot 4\text{H}_2\text{O}$, $\text{Mn}(\text{CH}_3\text{COO})_2 \cdot 4\text{H}_2\text{O}$, $\text{FeCl}_3 \cdot 6\text{H}_2\text{O}$, $\text{RuCl}_3 \cdot 3\text{H}_2\text{O}$, $\text{VOSO}_4 \cdot \text{H}_2\text{O}$ and $\text{UO}_2(\text{CH}_3\text{COO})_2$ with a suitable amount of a ligand ethanolic solution in molar ratio (1 metal : 2 ligand) in the presence of 2 mL of triethylamine. The reaction mixture was then refluxed for 3 hours. The formed precipitates were filtered off, washed with ethanol, then with diethyl ether and dehydrated under vacuum over anhydrous CaCl_2 . The same method was used to prepare complexes; (**2**), (**5-6**) and (**9**) but in molar ratio (1 metal : 1 ligand) using the following salts; $\text{Cu}(\text{CH}_3\text{COO})_2 \cdot \text{H}_2\text{O}$, $\text{Cu}(\text{NO}_3)_2 \cdot 3\text{H}_2\text{O}$, $\text{Ni}(\text{CH}_3\text{COO})_2 \cdot 4\text{H}_2\text{O}$ and $\text{Zn}(\text{CH}_3\text{COO})_2 \cdot 2\text{H}_2\text{O}$.

Copper(II) complex (2). $[\text{Cu}(\text{H}_2\text{L})(\text{CH}_3\text{COO})_2(\text{H}_2\text{O})_2]$, $\text{C}_{26}\text{H}_{30}\text{CuN}_6\text{O}_{10}$ (FW = 650.10), yield: 67%, m.p. > 300. Color: reddish brown, molar conductance (Λ) was $11.9 \Omega^{-1}\text{cm}^2\text{mol}^{-1}$. Elemental anal. calcd.: C, 48.04; H, 4.65; N, 12.93; Cu, 9.77; found: C, 48.19; H, 4.41; N, 12.49; Cu, 9.51; IR (KBr, cm^{-1}): 3426, $\nu(\text{H}_2\text{O})$, 3361 $\nu(\text{OH})$, 3255 $\nu(\text{NH}^{\text{I}})$, 3110 $\nu(\text{CH}_2\text{NH}^{\text{II}})$, 1694 $\nu(\text{C}=\text{O})$, 1604 $\nu(\text{C}=\text{N})$, 1470 $\nu(\text{N}=\text{N})$, 1280 $\nu(\text{C}-\text{OH})$, 1001 $\nu(\text{N}-\text{N})$, 578 $\nu(\text{Cu}-\text{O})$, 504 $\nu(\text{Cu}-\text{N})$, 1555 1370 ($\Delta = 185$) $\nu_{\text{s}}\text{CH}_3\text{COO}$, $\nu_{\text{as}}\text{CH}_3\text{COO}$.

Copper(II) complex (3). $[\text{Cu}(\text{H}_2\text{L})_2\text{Cl}_2] \cdot 2\text{H}_2\text{O}$, $\text{C}_{44}\text{H}_{44}\text{CuClN}_6\text{O}_{10}$ (FW = 1035.35), yield: 60%, m.p. > 300. Color: reddish brown, molar conductance (Λ) was $35.3 \Omega^{-1}\text{cm}^2\text{mol}^{-1}$. Elemental

anal. calcd.: C, 51.04; H, 4.28; N, 16.14; Cu, 6.41; found: C, 50.81.; H, 4.34; N, 16.19; Cu, 6.12; IR (KBr, cm^{-1}): 3424 $\nu(\text{H}_2\text{O})$, 3360 $\nu(\text{OH})$, 3254 $\nu(\text{NH}^{11})$, 3090 $\nu(\text{CH}_2\text{NH}^7)$, 1692 $\nu(\text{C}=\text{O})$, 1609 $\nu(\text{C}=\text{N})$, 1469 $\nu(\text{N}=\text{N})$, 1258 $\nu(\text{C}-\text{OH})$, 977 $\nu(\text{N}-\text{N})$, 589 $\nu(\text{Cu}\leftarrow\text{O})$, 511 $\nu(\text{Cu}\leftarrow\text{N})$.

Copper(II) complex (4). $[\text{Cu}(\text{HL})_2(\text{H}_2\text{O})_2]$, $\text{C}_{44}\text{H}_{42}\text{CuN}_{12}\text{O}_{10}$ (FW = 962.42), yield: 63%, m.p. > 300. Color: pale brown, molar conductance (Λ) was $9.5 \Omega^{-1}\text{cm}^2\text{mol}^{-1}$. Elemental anal. calcd.: C, 54.91; H, 4.40; N, 17.46; Cu, 6.60; found: C, 54.71.; H, 4.22; N, 17.39; Cu, 6.69; IR (KBr, cm^{-1}): 3420 $\nu(\text{H}_2\text{O})$, 3365 $\nu(\text{OH})$, 3105 $\nu(\text{CH}_2\text{NH}^7)$, 1607 $\nu(\text{C}=\text{N})$, 1549 $\nu(\text{N}=\text{C}-\text{O})$, 1475 $\nu(\text{N}=\text{N})$, 1289 $\nu(\text{C}-\text{O}^{10})$, 1257 $\nu(\text{C}-\text{O}_{\text{ph}})$, 975 $\nu(\text{N}-\text{N})$, 588 $\nu(\text{Cu}-\text{O})$, 498 $\nu(\text{Cu}\leftarrow\text{N})$.

Copper(II) complex (5). $[\text{Cu}(\text{L})(\text{H}_2\text{O})_3]$, $\text{C}_{22}\text{H}_{24}\text{CuN}_6\text{O}_7$ (FW = 548.01), yield: 59%, m.p. = 280. Color: brown, molar conductance (Λ) was $7.8 \Omega^{-1}\text{cm}^2\text{mol}^{-1}$. Elemental anal. calcd.: C, 48.22; H, 4.41; N, 15.34; Cu, 11.60; found: C, 48.20.; H, 4.61; N, 15.21; Cu, 11.36; IR (KBr, cm^{-1}): 3434 $\nu(\text{H}_2\text{O})$, 3129 $\nu(\text{CH}_2\text{NH}^7)$, 1608 $\nu(\text{C}=\text{N})$, 1588 $\nu(\text{N}=\text{C}-\text{O})$, 1467 $\nu(\text{N}=\text{N})$, 1377 $\nu(\text{C}-\text{O}^{10})$, 1270 $\nu(\text{C}-\text{O}_{\text{ph}})$, 976 $\nu(\text{N}-\text{N})$, 591 $\nu(\text{Cu}\leftarrow\text{O})$, 490 $\nu(\text{Cu}\leftarrow\text{N})$.

Nickel complex (6). $[\text{Ni}(\text{HL})(\text{CH}_3\text{COO})(\text{H}_2\text{O})_2]$, $\text{C}_{24}\text{H}_{26}\text{NiN}_6\text{O}_8$ (FW = 585.19), yield: 64%, m.p. > 300. Color: red, molar conductance (Λ) was $12.4 \Omega^{-1}\text{cm}^2\text{mol}^{-1}$. Elemental anal. calcd.: C, 49.26; H, 4.48; N, 14.36; Ni, 10.03; found: C, 48.80.; H, 4.60; N, 14.30; Ni, 10.17; IR (KBr, cm^{-1}): 3420 $\nu(\text{H}_2\text{O})$, 3099 $\nu(\text{CH}_2\text{NH}^7)$, 1605 $\nu(\text{C}=\text{N})$, 1581 $\nu(\text{N}=\text{C}-\text{O})$, 1469 $\nu(\text{N}=\text{N})$, 1372 $\nu(\text{C}-\text{O}^{10})$, 1268 $\nu(\text{C}-\text{O}_{\text{ph}})$, 987 $\nu(\text{N}-\text{N})$, 588, 545 $\nu(\text{Ni}-\text{O})$, 487 $\nu(\text{Ni}\leftarrow\text{N})$, 1543, 1343 ($\Delta = 200$) $\nu_s\text{CH}_3\text{COO}$, $\nu_{\text{as}}\text{CH}_3\text{COO}$.

Cobalt(II) complex (7). $[\text{Co}(\text{H}_2\text{L})_2(\text{CH}_3\text{COO})_2] \cdot 2\text{H}_2\text{O}$, $\text{C}_{48}\text{H}_{50}\text{CoN}_{12}\text{O}_{14}$ (FW = 1077.92), yield: 59%, m.p. > 300. Color: dark red, molar conductance (Λ) was $9.3 \Omega^{-1}\text{cm}^2\text{mol}^{-1}$. Elemental anal. calcd.: C, 53.48; H, 4.68; N, 15.59; Co, 5.47; found: C, 53.17.; H, 4.52; N, 16.01.60; Co, 5.31; IR (KBr, cm^{-1}): 3422 $\nu(\text{H}_2\text{O})$, 3360 $\nu(\text{OH})$, 3254 $\nu(\text{NH}^{11})$, 3115 $\nu(\text{CH}_2\text{NH}^7)$, 1691 $\nu(\text{C}=\text{O})$, 1609 $\nu(\text{C}=\text{N})$, 1467 $\nu(\text{N}=\text{N})$, 1258 $\nu(\text{C}-\text{OH})$, 997 $\nu(\text{N}-\text{N})$, 588 $\nu(\text{Co}\leftarrow\text{O})$, 505 $\nu(\text{Co}\leftarrow\text{N})$, 1562, 1374 ($\Delta = 188$) $\nu_s\text{CH}_3\text{COO}$, $\nu_{\text{as}}\text{CH}_3\text{COO}$.

Manganese(II) complex (8). $[\text{Mn}(\text{H}_2\text{L})_2(\text{CH}_3\text{COO})_2] \cdot 2\text{H}_2\text{O}$, $\text{C}_{48}\text{H}_{50}\text{MnN}_{12}\text{O}_{14}$ (FW = 1073.92), yield: 57%, m.p. > 300. Color: dark orange, molar conductance (Λ) was $7.5 \Omega^{-1}\text{cm}^2\text{mol}^{-1}$. Elemental anal. calcd.: C, 53.68; H, 4.69; N, 15.65; Mn, 5.12; found: C, 53.44.; H, 4.44; N, 15.41; Mn, 5.25; IR (KBr, cm^{-1}): 3434 $\nu(\text{H}_2\text{O})$, 3360 $\nu(\text{OH})$, 3110 $\nu(\text{CH}_2\text{NH}^7)$, 1691 $\nu(\text{C}=\text{O})$, 1608 $\nu(\text{C}=\text{N})$, 1473 $\nu(\text{N}=\text{N})$, 1258 $\nu(\text{C}-\text{O}_{\text{ph}})$, 966 $\nu(\text{N}-\text{N})$, 575 $\nu(\text{Mn}-\text{O})$, 489 $\nu(\text{Mn}\leftarrow\text{N})$, 1571, 1390 ($\Delta = 181$) $\nu_s\text{CH}_3\text{COO}$, $\nu_{\text{as}}\text{CH}_3\text{COO}$.

Zinc(II) complex (9). $[\text{Zn}(\text{HL})(\text{CH}_3\text{COO})(\text{H}_2\text{O})_2]$, $\text{C}_{24}\text{H}_{26}\text{ZnN}_6\text{O}_8$ (FW = 591.88), yield: 60%, m.p. > 300. Color: red, molar conductance (Λ) was $8.5 \Omega^{-1}\text{cm}^2\text{mol}^{-1}$. Elemental anal. calcd.: C, 48.70; H, 4.43; N, 14.20; Zn, 11.05; found: C, 48.22.; H, 4.56; N, 14.30; Zn, 11.19; IR (KBr, cm^{-1}): 3426 $\nu(\text{H}_2\text{O})$, 3140 $\nu(\text{NH}^7)$, 1615 $\nu(\text{C}=\text{N})$, 1587 $\nu(\text{N}=\text{C}-\text{O})$, 1473 $\nu(\text{N}=\text{N})$, 1375 $\nu(\text{C}-\text{O}^{10})$, 1262 $\nu(\text{C}-\text{OH})$, 1009 $\nu(\text{N}-\text{N})$, 600 $\nu(\text{Zn}\leftarrow\text{O})$, 507 $\nu(\text{Zn}\leftarrow\text{N})$, 1546, 1336 ($\Delta = 210$) $\nu_s\text{CH}_3\text{COO}$, $\nu_{\text{as}}\text{CH}_3\text{COO}$.

Iron(III) complex (10). $[\text{Fe}(\text{H}_2\text{L})_2\text{Cl}_2] \cdot \text{Cl}$, $\text{C}_{44}\text{H}_{40}\text{FeCl}_3\text{N}_{12}\text{O}_8$ (FW = 1027.1), yield: 55%, m.p. > 280. color: dark green, molar conductance (Λ) was $74.1 \Omega^{-1}\text{cm}^2\text{mol}^{-1}$. Elemental anal. calcd.: C, 51.45; H, 3.93; N, 16.37; Fe, 5.44; Cl, 10.36; found: C, 52.01.; H, 4.01; N, 16.50; Fe, 5.40; IR (KBr, cm^{-1}): 3359 $\nu(\text{OH})$, 3253 $\nu(\text{NH}^{11})$, 3110 $\nu(\text{CH}_2\text{NH}^7)$, 1692 $\nu(\text{C}=\text{O})$, 1610 $\nu(\text{C}=\text{N})$, 1486 $\nu(\text{N}=\text{N})$, 1257 $\nu(\text{C}-\text{OH})$, 967 $\nu(\text{N}-\text{N})$, 585 $\nu(\text{Fe}\leftarrow\text{O})$, 511 $\nu(\text{Fe}\leftarrow\text{N})$.

Ruthenium(III) complex (11). $[\text{Ru}(\text{H}_2\text{L})(\text{Cl}_2)\cdot\text{Cl}\cdot 2\text{H}_2\text{O}]$, $\text{C}_{44}\text{H}_{44}\text{RuCl}_3\text{N}_{12}\text{O}_{10}$ (FW = 1108.32), yield: 63%, m.p. = 264, color: dark green, molar conductance (Λ) was $91.5 \Omega^{-1}\text{cm}^2\text{mol}^{-1}$. Elemental anal. calcd.: C, 47.68; H, 4.00; N, 15.17; Ru, 9.12; found: C, 47.31.; H, 3.90; N, 14.88; Ru, 8.88; IR (KBr, cm^{-1}): 3359 $\nu(\text{NH})$, 3253 $\nu(\text{NH}^{11})$, 3110 $\nu(\text{CH}_2\text{NH}^7)$, 1692 $\nu(\text{C}=\text{O})$, 1613 $\nu(\text{C}=\text{N})$, 1485 $\nu(\text{N}=\text{N})$, 1271 $\nu(\text{C}-\text{OH})$, 967 $\nu(\text{N}-\text{N})$, 953 $\nu(\text{V}=\text{O})$, 561 $\nu(\text{Ru}\leftarrow\text{O})$, 511 $\nu(\text{Ru}\leftarrow\text{N})$.

Vanadyl complex (12). $[\text{VO}(\text{H}_2\text{L})_2(\text{SO}_4)]$, $\text{C}_{44}\text{H}_{40}\text{VN}_{12}\text{O}_{13}\text{S}$ (FW = 1027.87), yield: 51%, m.p. = 276, color: yellowish green, molar conductance (Λ) was $24.5 \Omega^{-1}\text{cm}^2\text{mol}^{-1}$. Elemental anal. calcd.: C, 51.41; H, 3.92; N, 16.35; V, 4.96; found: C, 51.31.; H, 3.83; N, 13.19; V, 4.81; IR (KBr, cm^{-1}): 3360 $\nu(\text{OH})$, 3253 $\nu(\text{NH}^{11})$, 3122 $\nu(\text{CH}_2\text{NH}^7)$, 1690 $\nu(\text{C}=\text{O})$, 1614 $\nu(\text{C}=\text{N})$, 1485 $\nu(\text{N}=\text{N})$, 1277 $\nu(\text{C}-\text{OH})$, 987 $\nu(\text{N}-\text{N})$, 571 $\nu(\text{V}\leftarrow\text{O})$, 510 $\nu(\text{V}\leftarrow\text{N})$.

Uranyl complex (13). $[\text{UO}_2(\text{H}_2\text{L})(\text{CH}_3\text{COO})_2]\cdot 2\text{H}_2\text{O}$, $\text{C}_{48}\text{H}_{50}\text{UN}_{12}\text{O}_{16}$ (FW = 1289.1), yield: 62%, m.p. > 300, color: orange, molar conductance (Λ) was $16.6 \Omega^{-1}\text{cm}^2\text{mol}^{-1}$. Elemental anal. calcd.: C, 44.73; H, 3.91; N, 13.04; U, 18.47; found: C, 44.41.; H, 4.03; N, 13.19; U, 18.00; IR (KBr, cm^{-1}): 3407 $\nu(\text{H}_2\text{O})$, 3360 $\nu(\text{OH})$, 3253 $\nu(\text{NH}^{11})$, 3115 $\nu(\text{CH}_2\text{NH}^7)$, 1664 $\nu(\text{C}=\text{O})$, 1609 $\nu(\text{C}=\text{N})$, 1472 $\nu(\text{N}=\text{N})$, 1257 $\nu(\text{C}-\text{OH})$, 966 $\nu(\text{N}-\text{N})$, 978 $\nu(\text{O}=\text{U}=\text{O})$, 575 $\nu(\text{U}\leftarrow\text{O})$, 508 $\nu(\text{U}\leftarrow\text{N})$, 1558, 1346 ($\Delta = 212$) $\nu_{\text{s}}\text{CH}_3\text{COO}$, $\nu_{\text{as}}\text{CH}_3\text{COO}$.

Microbicides activities

The antimicrobial liveliness of the prepared compounds were carried out by well diffusion method in the Department of Botany, microbiology lab, Faculty of Science, El-Menoufia University, Egypt [23]. *Escherichia coli* and *Aspergillus niger* were used for assaying the antimicrobial activities against the ligand and its complexes at 150, 200 and 250 $\mu\text{g}/\text{mL}$ concentrations in DMSO. Negative control used was DMSO. The bacterium and fungus strains were subcultured in nutrient agar and Czapek-Dox's, respectively. The media were subjected sterilizer by autoclaving at 121 $^\circ\text{C}$ for 15 min then let to cool to 45 $^\circ\text{C}$. Finally, the media were casting into Petri dishes of diameter 90 mm and incubated at 28 $^\circ\text{C}$. After solidify, Petri dishes were stored at 4 $^\circ\text{C}$ for few hours. Microorganisms were prevalence over each dish by sterile bent loop rod. Well were down by sterile cork borer. The resulted pits were sites for the tested compounds of known concentration. For comparison salts solution, standard drugs like tetracycline and amphotericin B were tested under identical conditions. Plates were let to stand in a refrigerator for two hours before incubation to let the diffusion of the tested compounds in the media. The Petri dishes were incubated for 48 h at 28 $^\circ\text{C}$ for fungus and at 37 $^\circ\text{C}$ for bacterium. The zone of inhibition was measured in millimeters accurately. All determinations were made three times for all compounds and the average was record.

RESULTS AND DISCUSSION

2-(*p*-Tolylamino) acetohydrazide reacted with 2-hydroxy-5-((4-nitrophenyl)diazonyl) benzaldehyde in EtOH by one mole to one mole, producing ligand (H_2L) (**1**), as shown in Scheme 1. The ligand (**1**) was reacted with metal salts in the presence of triethylamine (2 mL) in molar ratios (2:1) gave complexes; (**3-4**), (**7-8**) and (**10-13**) however, (1:1) gave complexes; (**2**), (**5-6**) and (**9**) with different structures. The prepared compounds are crystalline solids, colored and steady at 25 $^\circ\text{C}$ and do not decompose after protracted storage. The complexes are not soluble in H_2O , EtOH, MeOH, C_6H_6 , $\text{C}_6\text{H}_5\text{CH}_3$, MeCN and CHCl_3 , but soluble in dimethylformamide (DMF) or dimethyl sulfoxide (DMSO). Physical, elemental, spectral and XRD data were presented in experimental section and Tables 1-5 which are compliant with the

proposed structures as shown in Figures 1-3. The elemental data confirmed that the complexes (3-4), (7-8) and (10-13) were found to be formed in molar ratio 1:2, M:L but complexes (2), (5-6) and (9) were found to be formed in molar ratio 1:1, M:L.

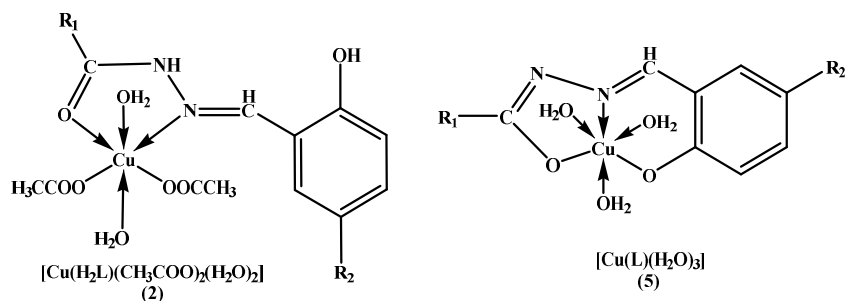


Figure 1. Structure representation of Cu(II) complexes (2, 5).

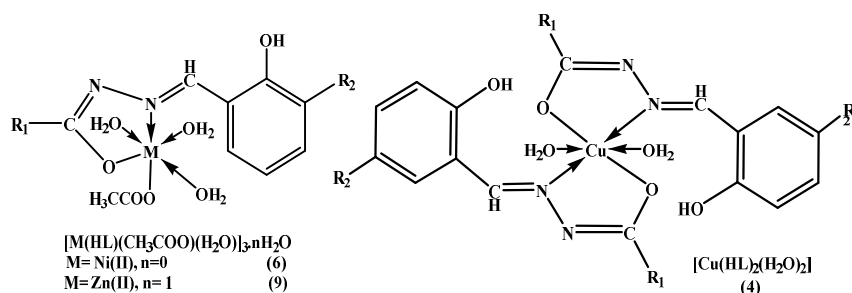


Figure 2. Structure representation of Cu^{2+} , Ni^{2+} and Zn^{2+} complex (4), (6) and (9).

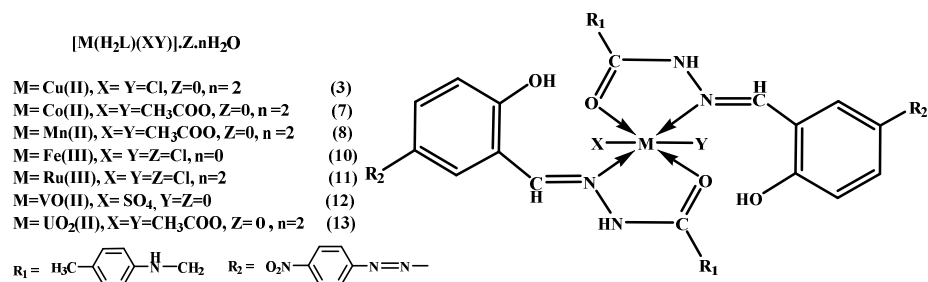


Figure 3. Structure representation of Cu^{2+} , Co^{2+} , Mn^{2+} , Fe^{3+} , Ru^{2+} , VO^{2+} and UO_2^{2+} complexes (3, 7-8 and 10-13).

¹H- and ¹³C-NMR spectra of the ligand

The ¹H-NMR spectrum of the ligand displayed chemical shifts which were compliant with the suggested structure. The spectrum of the ligand showed that the amino group signal (–NH₂) of hydrazide moiety was absent. The spectrum showed five sets of chemical shift, the singlets

observed at 11.5 (s, 1H), 11.8 (s, 1H) and 5.8 (s, 1H) ppm could be attributed to the protons of (OH²⁰), (NH¹¹) and (NH⁷), respectively [24-26]. The appearing of these proton resonances at high δ values could be due to their connection to extremely electronegative atoms oxygen and nitrogen. This assignment was assured by considerably decreasing intensity of these bands in the deuterated spectra. The situation of these signal in the downfield region indicates the probability of hydrogen bonding formation by these hydrogen atoms [26]. The second chemical shift spotted as singlet at 8.59 (s, 1H) ppm was referred to azomethine proton (H-C=N) [26, 27]. The third one spotted as multiples in the 6.5–8.4 (m, 11H) ppm range could be corresponded to aromatic protons. It was obvious from the ¹H-NMR spectrum of ligand the presence of the ligand in keto form only and no proof for the existence of enol form. This conclusion was established from the occurrence of the chemical shift of the (NH) and phenolic (OH) only and lack of the (OH) chemical shift of the enolic form. This result was reported by many authors [24, 26].

The ¹³C-NMR spectrum showed chemical shifts at 172, 167.9, 148.5 and 146.5 ppm belong to C=O, –C-OH, C-NH and CH=N- groups, respectively [27, 28]. The chemical shift at 161 and 155 ppm may be belong to C-N=N-C group [27]. However the chemical shift in the 113-145.7 ppm range referred to the aromatic carbon [28]. The chemical shift appeared at 40.52 and 21.5 ppm could be belong to –CH₂-N and CH₃ groups, respectively [29].

Conductivity measurements

The molar conductance of complexes (2-9) and (13) (1×10^{-3} M, DMF at 25 °C) were in the 7.5–35.4 $\Omega^{-1}\text{cm}^2\text{mol}^{-1}$ range indicating that these complexes are non-electrolytic [30]. These confirmed that the anions of these complexes were chelated to metal ion. The considerable high values of some complexes could be attributable to the partial solvolysis by DMF [30]. The molar conductivity of complexes (10) and (11) were 74.1 and 91.5 $\Omega^{-1}\text{cm}^2\text{mol}^{-1}$, respectively, referring the electrolytic behavior of these complexes. This result is proposed with Greenwood *et al.* Studies [48]. They have proposed 50–70 $\Omega^{-1}\text{cm}^2\text{mol}^{-1}$ as the range for 1:1 electrolyte [31].

IR spectra

The spectrum of the ligand (H₂L) displayed a medium peak at 3253 cm^{-1} could be referred to $\nu(\text{NH}^{11})$ group, whereas the strong peak at 1692 cm^{-1} belongs the carbonyl group of the hydrazide moiety [25]. This observation indicated that in the solid state, the H₂L is existing in the ketonic form [32]. In addition the presence of a sharp band at 3360 cm^{-1} could be referred to the stretching vibration of the phenolic hydroxy group [25]. The comparatively strong and medium peaks which lying at 3130, 1613, 1470 and 954 cm^{-1} corresponded to the amine (CH₂-NH⁷), azomethine [33], azo [34], and $\nu(\text{N-N})$ [32] groups, respectively. The peak appeared at 1260 cm^{-1} is belong to the phenolic moiety [32]. The mode of bonding of the ligand can be predicted by comparing the IR spectra of the complexes with the ligand. The IR spectral data obtained for complexes displayed that the ligand behaves as either of the following:

(1) Neutral bidentate as in case of complexes (2-3), (7-8) and (10-13) in which the ligand chelated to metal ions via ketonic carbonyl oxygen and azomethine nitrogen atoms. This behavior of coordination was supported by the next proofs: (i) the peak characteristic to $\nu(\text{NH}^{11})$ was exist yet and the carbonyl group frequency is lowered or appeared as medium intensity indicating that, the ligand chelated to metal ion via ketonic carbonyl oxygen; (ii) the band characteristic to azomethine group $\nu(\text{C=N})$ shifted and appeared as week band in the 1614-1604 cm^{-1} . Simultaneously, the peak belongs to $\nu(\text{N-N})$ was shifted to a higher frequency and appearing in the 966-1001 cm^{-1} range. The increment in the frequency of this peak is an obvious reference to the increasing in the double bond property is off-setting the lack of electron density

through electron donation to the metal ions and further confirmed that the azomethine group participate in the chelation [33].

(2) Dibasic tridentate as in complex (5) in which the ligand bonded to the copper ion through the enolic carbonyl oxygen (C-O), deprotonated hydroxyl oxygen and azomethine nitrogen (C=N) atoms. This bonding behavior was supported by the next: (i) the peaks characteristic to the carbonyl and $\nu(\text{NH})$ groups vanished referring that, the H_2L bonded via enolic carbonyl oxygen atom, which is furthermore confirming by the occurrence of new peaks at 1588, 1377 cm^{-1} referring to the $\nu(\text{N}=\text{C}-\text{O})$, and $\nu(\text{C}-\text{O})$, respectively [34]. (ii) The peak characteristic to $\nu(\text{C}=\text{N})$ group lowered to 1608 where the peak belongs $\nu(\text{N}-\text{N})$ shifted to a higher frequency and appearing at 976 cm^{-1} . The increment in the frequency of $\nu(\text{N}-\text{N})$ bond is an obvious reference to the increasing in the double bond property is off-setting the lack of electron density via electron donation to the metal ions and further confirmed that the azomethine group takes part in the chelation [33]. (iii) The shifting in the peak characteristic to phenolic hydroxy group and disappearing of the peak assigned to hydroxyl proton indicating that the deprotonated phenolic oxygen atom participates in the bonding.

(3) Monobasic bidentate as in complex (4), (6) and (9) in which the ligand bonded to the metal ions through the enolic carbonyl oxygen (C-O), and azomethine nitrogen (C=N) atoms. This bonding behavior was confirmed by: (i) the bands characteristic to the carbonyl $\nu(\text{C}=\text{O})$, and $\nu(\text{NH})$ groups vanished referring that the H_2L bonded in its enolic form via enolic carbonyl oxygen, which is further assured by the occurrence of new peaks in the 1588-1549, 1289-1325 cm^{-1} ranges attributing to the $\nu(\text{N}=\text{C}-\text{O})$, and $\nu(\text{C}-\text{O})$, respectively [35]. (ii) The characterized frequency of the azomethine group lowered whereas the characterized frequency of $\nu(\text{N}-\text{N})$ increases and appearing in the 975-1009 cm^{-1} range. The increment in the frequency of $\nu(\text{N}-\text{N})$ band is an obvious reference to the increasing in the double bond property is off-setting the lack of electron density via electron donation to the metal ions and further confirmed that the azomethine group participate in the chelation process [33]. The occurrence of new peaks in the 561-600 and 489-511 cm^{-1} ranges for all complexes could be attributed to the $\nu(\text{M}-\text{O})$, $\nu(\text{M} \leftarrow \text{O})$ and $\nu(\text{M} \leftarrow \text{N})$, respectively [36]. These peaks confirm that linkage between ligand and metal ions occurred via oxygen atoms of the enolic or ketonic carbonyl and/or deprotonated phenolic hydroxyl groups as well as azomethine nitrogen atom. The IR spectrum of the sulfate complex (12) displayed the appearance of new bands at 1237, 1143, 1058, 888 cm^{-1} . These bands indicate that the sulfate ion is coordinated to vanadyl ion as chelating unidentate fashion [37, 38]. In acetate complexes, the acetate ion may be coordinate to the metal ion in unidentate, bidentate or bridging bidentate behavior. The $\nu_{\text{as}}(\text{CO}_2)$ and $\nu_{\text{s}}(\text{CO}_2)$ of the free acetate ion are ca. 1560 and 1416 cm^{-1} , respectively. In unidentate acetate complexes $\nu(\text{C}=\text{O})$ is higher than $\nu_{\text{s}}(\text{CO}_2)$ and $\nu(\text{C}-\text{O})$ is lower than $\nu_{\text{as}}(\text{CO}_2)$. As a consequence the isolation between the two $\nu(\text{CO})$ is higher in unidentate than in free ion but in bidentate the isolation is lower than in the free ion whilst in bridging bidentate the two $\nu(\text{CO})$ is closer to the free ion [38]. In complexes (2), (6-9) and (13), the presence of two new peaks in the 1546-1571 and 1336-1374 cm^{-1} ranges are imputed to the symmetric and asymmetric stretching vibration of the acetate group. The coordination mode of acetate group was deduced from the value of the observed separation (Δ) between the $\nu_{\text{as}}(\text{COO})$ and $\nu_{\text{s}}(\text{COO})$. The (Δ) values between $\nu_{\text{as}}(\text{COO})$ and $\nu_{\text{s}}(\text{COO})$ in (2), (6-9) and (13) complexes were in the 181-212 cm^{-1} range supporting the coordination of acetate group in a monodentate fashion [38-40]. The IR spectra of the VO_2^{2+} and UO_2^{2+} complexes implied a peak at 953 and 978 cm^{-1} which could be imputed to $\nu(\text{V}=\text{O})$ and $\nu(\text{O}=\text{U}=\text{O})$ [41].

Magnetic moment

The magnetic moments (μ_{eff}) of (2-8) and (10-12) complexes at room temperature were collected in Table 1. The μ_{eff} values showed that the (2-8) and (10-12) complexes are

paramagnetic. The Cu^{2+} complexes (**2-5**) show μ_{eff} values in the 1.70–1.75 BM range which are compatible with one unpaired electron Cu^{2+} in octahedral environment [24]. Ni^{2+} complex (**6**) shows μ_{eff} value 2.85 BM which is compatible with two unpaired electrons system of octahedral Ni^{2+} complex [42]. Co^{2+} complex (**7**) shows value 3.98 BM, indicating a high spin Co^{2+} complex [43]. The μ_{eff} values of Mn^{2+} and Fe^{3+} complexes (**8**) and (**10**) are 5.67 and 5.90 BM, respectively, which was indication to five unpaired electrons system of octahedral Mn^{2+} and Fe^{3+} complexes. The μ_{eff} value of Ru^{3+} complex (**11**) is 1.68 BM which is characteristic to d^5 low spin Ru^{3+} complex [35]. VO^{2+} complex (**12**) shows μ_{eff} value 1.70 BM which is corresponding to one unpaired electron [35, 37].

Electronic absorption spectra

Table 1 showed the electronic spectral data of compounds (**1-13**) in DMF solutions. The ligand structure reveals that, the azo group lone pairs of electrons are not the only interacting non-bonding electrons. Since hydrazone moiety is additional sources of lone pair of electrons (nitrogen and oxygen atoms). Thus, other $n \rightarrow \pi^*$ transition is predictable to take place from these non-bonding orbitals to various molecular orbital extending over such a big molecule [44]. The data revealed that, the ligand comprised many peaks in the UV and visible regions. The shortest wavelength peaks observed at 225 and 245 nm could be assignable to $\pi \rightarrow \pi^*$ transitions of the benzenoid and intra-ligand [28, 33]. Whereas the bands appeared at 320 and 335 nm could be imputed to $n \rightarrow \pi^*$ transitions of carbonyl and azomethine groups [24]. The bands situated at 370 nm could be corresponded to $\pi \rightarrow \pi^*$ transition including the π electron of the azo group [44]. The peak situated at 420 nm could be imputed to $\pi \rightarrow \pi^*$ transition including the whole electronic system of the compounds with a considerable charge transfer character emerging fundamentally from the phenolic moiety [44]. The electronic spectrum of Cu^{2+} complexes (**2-5**) display three peaks centered in the 460-490, 540-570, 620-690 nm ranges. These bands assigned to $(v_3)^2B_{1g} \rightarrow ^2E_g$, $(d_{x^2-y^2} \rightarrow d_{xy})$, $(v_2)^2B_{1g} \rightarrow ^2B_{2g}$ ($d_{x^2-y^2} \rightarrow d_{yz}, d_{xz}$), $(v_1)^2B_{1g} \rightarrow ^2A_{1g}$ ($d_{x^2-y^2} \rightarrow d_{z^2}$) transitions which indicated that the Cu^{2+} complexes have tetragonally distorted octahedral geometry (Figures 1-3) [45, 46]. Ni^{2+} complex (**6**) exhibited three bands located at 510, 610, 890 nm which could be imputed to $(v_3)^3A_{2g}(F) \rightarrow ^3T_{1g}(P)$, $(v_2)^3A_{2g}(F) \rightarrow ^3T_{1g}(F)$, $(v_1)^3A_{2g}(F) \rightarrow ^3T_{2g}(F)$ spin allowed transitions, which are characteristic to Ni^{2+} ion in an octahedral structure (Figure 2) [45, 47]. The v_2/v_1 ratio for this complex is 1.46 which is lower than the regular range (1.5-1.75), referring that Ni^{2+} complex has a distorted octahedral geometry [47]. The Co^{2+} complex (**7**) showed bands at 540, 610, 980 nm, which could imputed to $(v_3)^4T_{1g}(F) \rightarrow ^4T_{2g}(P)$, $(v_2)^4T_{1g}(F) \rightarrow ^4A_{2g}(F)$ $(v_1)^4T_{1g}(F) \rightarrow ^4T_{2g}(F)$ transitions, respectively, referring to high spin Co^{2+} octahedral complex (Figure 3) [35, 45]. The v_2/v_1 ratio for the complex is 1.61 which is lower than the regular range (1.95–2.48), referring that Co^{2+} complex has a distorted octahedral geometry [47]. Mn^{2+} complexes (**8**) displays weak absorption bands at 510, 650 and 780 nm assigned to $^6A_{1g} \rightarrow ^4T_{1g}(4G)(v_1)$, $^6A_{1g} \rightarrow ^4E_g(4G)(v_2)$, $^6A_{1g} \rightarrow ^4E_g(4D)(v_3)$ and $^6A_{1g} \rightarrow ^4T_{1g}(4p)(v_4)$, respectively, characteristic to Mn^{2+} in octahedral geometry (Figure 3) [45, 48]. Fe^{3+} complex (**10**) gave bands at 570, 650 nm which due to $^6A_{1g} \rightarrow ^4T_{2g}$ and $^6A_{1g} \rightarrow ^4T_1(G)$ transitions. These peaks are distinctive of octahedral Fe^{3+} complex (Figure 3) [45, 49]. However, the electronic absorption spectrum of Ru^{3+} complex (**11**) displayed two peaks at 580 and 650 nm. The first peak is owing to LMCT transition while the last is imputed to $^2T_{2g} \rightarrow ^2A_{2g}$ transition. The peaks position is analogous to those observed for other octahedral Ru^{3+} complex (Figure 3) [45, 50]. The spectrum of VO^{2+} complex (**12**) showed that there are three bands at 490, 595, 615 nm that could be referred to $^2B_2(d_{xy}) \rightarrow ^2E(d_{xz}, d_{yz})$, $^2B_2(d_{xy}) \rightarrow ^2B_1(d_{x^2-y^2})$ and $^2B_2(d_{xy}) \rightarrow A_1(d_{z^2})$ transitions revealing that, the VO^{2+} complex has a distorted octahedral geometry (Figure 3) [45, 51]. The diamagnetic complexes Zn^{2+} complex (**9**) has d^{10} system, so they do not show d-d transitions. The bands observed are due to intra-ligand

transitions. The UO_2^{2+} complex (**13**) displays one peak at 500 nm referred to ligand to uranium charge transfer [50].

Table 1. UV-Vis. spectra of the ligand (H_2L) and its metal complexes.

No.	Bands in DMF	Electronic transition	μ_{eff} (BM)	Geometry
1	215, 250, 310, 370, 390	---	--	--
2	230, 290, 330, 380, 420, 490, 570, 630	$(\nu_3)^2\text{B}_{1g} \rightarrow ^2\text{E}_g$, $(d_{x^2-y^2} \rightarrow d_{xy})$ $(\nu_2)^2\text{B}_{1g} \rightarrow ^2\text{B}_{2g}$ $(d_{x^2-y^2} \rightarrow d_{yz}, d_{xz})$ $(\nu_1)^2\text{B}_{1g} \rightarrow ^2\text{A}_{1g}$ $(d_{x^2-y^2} \rightarrow d_{z^2})$	1.75	tetragonal distorted octahedral
3	250, 305, 330, 400, 470, 560, 620		1.70	
4	240, 300, 330, 390, 410, 460, 540, 690		1.71	
5	235, 300, 335, 390, 405, 460, 565, 650		1.73	
6	230, 300, 360, 395, 410, 510, 610, 890	$(\nu_3)^3\text{A}_{2g}(\text{F}) \rightarrow ^3\text{T}_{1g}(\text{P})$, $(\nu_2)^3\text{A}_{2g}(\text{F}) \rightarrow ^3\text{T}_{1g}(\text{F})$ $(\nu_1)^3\text{A}_{2g}(\text{F}) \rightarrow ^3\text{T}_{2g}(\text{F})$	2.85	distorted octahedral
7	225, 240, 300, 340, 400, 540, 670, 930	$(\nu_3)^4\text{T}_{1g}(\text{F}) \rightarrow ^4\text{T}_{2g}(\text{P})$, $(\nu_2)^4\text{T}_{1g}(\text{F}) \rightarrow ^4\text{A}_{2g}(\text{F})$ $(\nu_1)^4\text{T}_{1g}(\text{F}) \rightarrow ^4\text{T}_{2g}(\text{F})$	3.98	Distorted octahedral
8	255, 280, 300, 400, 510, 650, 780	$(\nu_1)^6\text{A}_{1g} \rightarrow ^4\text{T}_{1g}(4\text{G})$, $(\nu_2)^6\text{A}_{1g} \rightarrow ^4\text{E}_g(4\text{G})$ $(\nu_3)^6\text{A}_{1g} \rightarrow ^4\text{E}_g(4\text{D})$, $(\nu_4)^6\text{A}_{1g} \rightarrow ^4\text{T}_{1g}(4\text{P})$	5.67	Distorted octahedral
9	250, 330, 340, 390, 420, 460	Intraligand transitions	Dia.	--
10	240, 280, 300, 385, 420, 490, 570, 650	$^6\text{A}_{1g} \rightarrow ^4\text{T}_{2g}$ and $^6\text{A}_{1g} \rightarrow ^4\text{T}_1(\text{G})$	5.90	octahedral
11	250, 280, 350, 390, 415, 450, 580, 650	$^2\text{T}_{2g} \rightarrow ^2\text{A}_{2g}$	1.68	octahedral
12	220, 280, 350, 380, 400, 595, 615	$^2\text{B}_2(d_{xy}) \rightarrow \text{A}_1(d_{z^2})$, $\text{B}_2(d_{xy}) \rightarrow ^2\text{B}_1(d_{x^2-y^2})$, $^2\text{B}_2(d_{xy}) \rightarrow ^2\text{E}(d_{xz}, d_{yz})$	1.70	Distorted octahedral
13	250, 330, 340, 390, 420, 500	Ligand \rightarrow uranium	Dia	--

X-ray powder diffraction analysis

X-ray powder diffraction analysis of complexes (**2**) and (**3**) was performed to define the type of crystal system, lattice parameters, and the cell volume. The XRD patterns point out that these complexes have a crystalline nature. Indexing of the diffraction patterns was carried out using Ultima IV multipurpose diffraction system Plus Chekcell software. The Miller indices (hkl) along with observed and calculated 2θ angles, d values, and relative intensities of these complexes are recorded in Tables 2 and 3.

From the indexed data, the unit cell parameters were also calculated and are recorded in Table 4. The powder XRD patterns of complexes (**2-3**) are totally different from that of the starting materials, confirming the formation of complexes. It is found that the samples have monoclinic structures. The crystal structures of analogous type of samples were known as monoclinic and orthorhombic [52]. Furthermore, using the diffraction data, the mean crystallite sizes of the complexes, D , were determined according to the Scherer equation ($D = 0.9\lambda/(\beta \cos\theta)$), where λ is X-ray wavelength (1.5406 Å), θ is Bragg diffraction angle, and β is the full width at

half maximum of the diffraction peak. The average crystallite sizes of the two complexes were found to be 77.83 and 40.45 nm and the values are given in Table 4.

Table 2. Miller indices (*hkl*), observed, calculated 2θ angles, *d* values, and relative intensities for complex (2).

Peak No.	H	K	L	2Th(obs)	2Th(calc)	d sp. Å	Rel. int.
1	0	2	4	27.97	27.978	3.1874	20
2	-4	2	1	28.09	28.045	3.174	17
3	4	1	3	37.43	37.443	2.4007	100
4	-4	5	0	37.62	37.631	2.389	74
5	5	1	3	43.64	43.615	2.0724	59
6	-1	4	6	43.87	43.859	2.062	30
7	-6	4	8	63.82	63.82	1.4572	18
8	-6	6	7	64.12	64.119	1.4512	33
9	10	4	1	76.96	76.974	1.2379	45
10	-8	6	8	77.12	77.127	1.2357	40
11	-5	13	0	81.2	81.198	1.1836	24
12	3	4	10	81.32	81.321	1.1822	28

Table 3. Miller indices (*hkl*), observed, calculated 2θ angles, *d* values, and relative intensities for complex (3).

Peak No.	H	K	L	2Th(obs)	2Th(calc)	d sp. Å	Rel. int.
1	-1	4	2	23.43	23.428	3.7937	10
2	-1	3	3	23.55	23.547	3.7746	9
3	-2	4	2	25.38	25.365	3.5064	23
4	2	3	2	25.49	25.48	3.4916	19
5	2	4	1	25.63	25.631	3.4728	12
6	-1	2	4	26.26	26.27	3.3909	9
7	3	0	2	26.54	26.528	3.3558	20
8	1	5	1	26.82	26.798	3.3214	11
9	-1	4	4	31.47	31.472	2.8404	34
10	3	1	3	31.62	31.629	2.8273	37
11	-4	2	4	33.54	33.539	2.6697	14
12	-4	4	0	33.69	33.709	2.6581	16
13	-2	6	2	33.83	33.844	2.6474	14
14	-4	2	5	37.51	37.508	2.3957	100
15	-6	2	4	43.72	43.714	2.0688	35
16	-3	1	10	63.91	63.909	1.4554	13
17	-6	2	9	64.16	64.162	1.4503	10
18	0	4	11	77.12	77.12	1.2357	51
19	-2	15	1	81.28	81.282	1.1827	30

Table 4. The average crystallite sizes of complexes (2) and (3).

No.	Lattice parameters				Volume in (Å ³)	Crystal size <i>D</i> (nm)	Crystal system
	a (Å)	b (Å)	c (Å)	β [°]			
2	13.687	17.189	14.142	103.97	3228.87	77.83	Monoclinic
3	13.620	18.027	14.634	105.00	3470.57	40.45	Monoclinic

Thermogravimetric analysis (TGA)

Since the IR spectra indicated that the complexes molecules contain water molecules, thermal analysis (TG) was carried out to sure their kind. The TG curves of complexes showed peaks within the range 75–220 °C, for all complexes except (10) and (12) confirmed that these complexes have hydrated and/or coordinated water molecules. The complexes (2), (7) and (8)

decayed in three steps. The stage occurred in the 110-195 °C range with 5.90, 3.21 and 3.33% weight loss (calcd. 5.54, 3.34 and 3.35%) due to the removal of coordinated water molecule (2H₂O), respectively. The next step occurred in the 280-360 °C range with 17.65, 11.05, 10.77% weight loss (calcd. 18.15, 10.95 and 10.99%) due to elimination of acetate ions (2CH₃COOH) group from the complexes, respectively. The third step occurred in the 420-580 °C range with 63.04, 76.1 and 78.3% weight loss (calcd. 64.08, 78.76 and 79.06%), referring to whole degeneracy of complexes ending with metal oxides formation. Complex (3) decomposed in three steps. The first step happened at 80 °C with 3.30% weight loss (calcd. 3.48%) owing to removal of hydrated water (2H₂O). Second step occurred at 220-310 °C range with 6.62% weight loss (calcd 6.86%) owing to removal of chloride ions (2HCl). The third step occurred at 430-560 °C with 78.5% weight loss (calcd. 82%), refers to the whole degeneracy of the complex which finished with the formation CuO. Complexes (4) and (5) decomposed in two steps. The first step occurred at 190-220 °C with 3.91, 9.71% weight loss (calcd. 3.74 and 9.85%) due to elimination of coordinated water molecule (2H₂O or 3H₂O), respectively. The second step occurred at 400-580 °C with 85.1 and 76.01% weight loss (calcd. 87.99 and 75.63%) of the two complexes respectively corresponding to the whole degeneracy of the complexes which finished with the formation of CuO. Complexes (6) and (9) decayed in three stages. The first stage occurred in the 75-100 °C range with 6.25, 6.08% weight loss (calcd. 6.09 and 6.16%) due to elimination of hydrated water (2H₂O), respectively. The second step occurred at 170-230 °C range with 9.81 and 9.69% weight loss (calcd 10.08 and 9.97%) due to elimination of acetate ion (CH₃COOH). The third step occurred at 400-550 °C with 72.10 and 71.39% weight loss (calcd 71.00 and 70.19%), refers to the whole degeneracy of the complexes which finished with the formation NiO and ZnO, respectively. Complex (10) decomposed in two stages. First stage on occurred at 200-270 °C range with 11.11% weight loss (calcd 10.86%) owing to elimination of chloride ions (3HCl). Second stage occurred at 460-620 °C with 78.93% weight loss (calcd 81.87%) corresponding to the complete decomposition of the complexes which ended with the formation Fe₂O₃. Complex (11) decayed in three stages. First stage took place at 65-90 °C range with 3.49% weight loss (calcd. 3.25%) owing to elimination of hydration water molecule (2H₂O). The second stage occurred at 250-310 °C range with 9.34% weight loss (calcd. 9.60%) due to elimination of chloride ions (3HCl). The third step occurred at 490-620 °C with 76.33% weight loss (calcd. 75.87%) referring to the whole degeneracy of the complex which finished with the formation Ru₂O₃.

Antibacterial and antifungal screening

The free ligand and its Zn²⁺, Cu²⁺, Ni²⁺, Co²⁺, Mn²⁺, Fe³⁺, Ru³⁺, VO²⁺ and UO₂²⁺ complexes have been examined *in vitro* for their antibacterial and antifungal activities at different concentration using well diffusion method against *E. Coli* and *A. niger*. The obtained results were presented in Table 5. It is clear that, the activities of the prepared complexes increase with increasing the concentration of the solutions while at concentration 150 µg/mL the ligand and its complexes were inactive against *E. coli* and *A. niger*. All the metal complexes are more potent bactericides and fungicides than the ligand and the complexes were more active against fungi than bacteria. The results show that, complex (9) exhibited higher antifungal activity, complex (10) exhibited higher antibacterial than the rest complexes. The order of antifungal activity at 250 µg/mL for the compounds was, (9) > (10) > (8) > (12) > (6) > (3) = (4) = (7) = (11) > (5). While the order of antibacterial activity for the compounds at 250 µg/mL was (4) > (10) > (5) = (8) > (ligand) = (3) = (9) > (6) = (7) > (12) > (2) = (11). This growing in the activity could be expounded based on the chelation theory [53]. Chelation decrease the polarity of the metal ion extremely, fundamentally due to the partial involvement of its positive charge with donor groups and possible π -electron delocalization overall chelate ring. The lipid and polysaccharides are some important constituents of cell walls and membranes, which are favorable for metal ion

interaction. As well, the cell wall also contains many amino phosphates, carbonyl and cysteinyl ligands, which protect the integrity of the membrane by acting as diffusion barrier and provides appropriate sites for binding. Chelation can diminish not only the polarity of the metal ion, but also can raise the lipophilic property of the chelate and the interaction between metal ions and the lipid is preferable. This could lead to the slump of the permeability barrier of the cell resulting in interference with the normal cell processes. If the geometry and charge distribution around the molecule are incompatible with geometry and charge distribution around the pores of the bacterial cell wall, penetration through the wall by the toxic agent cannot take place and this will prevent the toxic reaction within the pores. Chelation is not the only criterion for the antimicrobial activity. Some important factors such as the nature of the metal ion, nature of the ligand, coordinating sites, and geometry of the complex, concentration, hydrophobicity, lipophilicity and presence of co-ligands have considerable influence on antimicrobial activity. Certainly, steric and pharmacokinetic factors also play a decisive role in deciding the potency of an antimicrobial agent.

Table 5. The inhibition zone (mm) of the ligand and its metal complexes on microorganisms at different concentrations.

Comp. No.	250 µg/mL		200 µg/mL	
	<i>A. niger</i>	<i>E. coli</i>	<i>A. niger</i>	<i>E. coli</i>
DMSO	0	0	0	0
Tetracycline	0	28	0	20
Amphotricene B	23	0	17	0
Ligand	0	12	0	7
2	0	9	0	6
3	19	12	12	6
4	19	16	11	8
5	18	13	11	9
6	20	11	11	7
7	19	11	11	5
8	23	13	13	7
9	26	12	16	9
10	24	17	12	8
11	19	9	9	0
12	22	11	12	4

CONCLUSION

In this paper a new azohydrazone ligand, 2-hydroxy-5-((4-nitrophenyl) diazenyl) benzyldene)-2-(*p*-tolylamino) acetohydrazide and its Zn²⁺, Cu²⁺, Ni²⁺, Co²⁺, Mn²⁺, Fe³⁺, Ru³⁺, VO₂²⁺ and UO₂²⁺ complexes were synthesized and characterized. The structures of the isolated complexes were interpreted by analytical techniques like elemental and thermogravimetric analyses, molar conductance, magnetic susceptibility measurements as well as spectroscopic techniques like UV-Visible, IR, ¹H and ¹³C NMR and X-ray diffraction. It is obvious from this study that six-membered rings were formed in which the ligand act either as tridentate NO₂ or bidentate NO donors leading to the formation complexes having octahedral or distorted octahedral geometry. The bioactivities of the ligand and its complexes against *E. coli* and *A. niger* by well diffusion method were evaluated. It is obvious from this bioactivity study that the complexes are more active than ligand and more active against fungicides than bactericides.

REFERENCES

1. Yaul, A.R.; Dhande, V.V.; Pethe, G.B.; Aswar, A.S. Synthesis, characterization, biological and electrical conductivity studies of some Schiff base metal complexes. *Bull. Chem. Soc. Ethiop.* **2014**, *28*, 255-264.
2. Shelke, V.A.; Jadhav, S.M.; Shankarwar, S.G.; Munde, A.S.; Chondhekar, T.K. Synthesis, characterization, antibacterial and antifungal studies of some transition and rare earth metal complexes of N-benzylidene-2-hydroxybenzohydrazide. *Bull. Chem. Soc. Ethiop.* **2011**, *25*, 381-391.
3. Altntop, M.D.; Özdemir, A.; Turan-Zitouni, G.; Ilgin, S.; Atli, Ö.; İçsan, G.; Kaplancikli, Z.A. Synthesis and biological evaluation of some hydrazone derivatives as new anticandidal and anticancer agents. *Eur. J. Med. Chem.* **2012**, *58*, 299-307.
4. Xu, J.; Zhou, T.; Xu, Z.-Q.; Gu, X.-N.; Wu, W.-N.; Chen, H.; Wang, Y.; Jia, L.; Zhu, T.-F.; Chen, R.-H. Synthesis, crystal structures and antitumor activities of copper(II) complexes with a 2-acetylpyrazine isonicotinoyl hydrazone ligand. *J. Mol. Struct.* **2017**, *1128*, 448-454.
5. Netalkar, P.P.; Netalkar, S.P.; Budagumpi, S.; Revankar, V.K. Synthesis, crystal structures and characterization of late first row transition metal complexes derived from benzothiazole core: Anti-tuberculosis activity and special emphasis on DNA binding and cleavage property. *Eur. J. Med. Chem.* **2014**, *79*, 47-56.
6. Gökçe, M.; Utku, S.; Küpeli, E. Synthesis and analgesic and anti-inflammatory activities 6-substituted-3(2H)-pyridazinone-2-acetyl-2-(*p*-substituted/nonsubstituted benzal)hydrazone derivatives. *Eur. J. Med. Chem.* **2009**, *44*, 3760-3764.
7. Kaushik, D.; Khan, S.A.; Chawla, G.; Kumar, S. N'-[(5-chloro-3-methyl-1-phenyl-1H-pyrazol-4-yl)methylene] 2/4-substituted hydrazides: Synthesis and anticonvulsant activity. *Eur. J. Med. Chem.* **2010**, *45*, 3943-3949.
8. Sangshetti, J.N.; Shaikh, R.I.; Khan, F.A.K.; Patil, R.H.; Marathe, S.D.; Gade, W.N.; Shinde, D.B. Synthesis, antileishmanial activity and docking study of N'-substitutedbenzylidene-2-(6,7-dihydrothieno[3,2-c]pyridin-5(4H)-yl) acetohydrazides. *Bioorg. Med. Chem. Lett.* **2014**, *24*, 1605-1610.
9. Özturan Özer, E.; Unsal Tan, O.; Ozadali, K.; Küçükkilinç, T.; Balkan, A.; Uçar, G. Synthesis, molecular modeling and evaluation of novel N'-2-(4-benzylpiperidin-/piperazin-1-yl)acylhydrazone derivatives as dual inhibitors for cholinesterases and Aβ aggregation. *Bioorg. Med. Chem. Lett.* **2013**, *23*, 440-443.
10. Shabbir, A.; Shahzad, M.; Ali, A.; Zia-Ur-Rehman, M. Anti-arthritis activity of N'-[(2,4-dihydroxyphenyl)methylidene]-2-(3,4-dimethyl-5,5-dioxidopyrazolo[4,3-c][1,2]benzothiazin-1(4H)-yl)acetohydrazide. *Eur. J. Pharmacol.* **2014**, *738*, 263-272.
11. Datta, A.; Liu, P.-H.; Huang, J.-H.; Garribba, E.; Turnbull, M.; MacHura, B.; Hsu, C.-L.; Chang, W.-T.; Pevec, A. End-to-end thiocyanato-bridged zig-zag polymers of Cu II, Co II and Ni II with a hydrazone ligand: EPR, magnetic susceptibility and biological study. *Polyhedron* **2012**, *44*, 77-87.
12. El-Gammal, O.A.; Elmorsy, E.A.; Sherif, Y.E. Evaluation of the anti-inflammatory and analgesic effects of Cu(II) and Zn(II) complexes derived from 2-(naphthalen-1-yloxy)-N'-(1-(pyridin-2-yl) ethylidene) acetohydrazide. *Spectrochim. Acta Part A Mol. Biomol. Spectrosc.* **2014**, *120*, 332-339.
13. Hayat, F.; Salahuddin, A.; Zargan, J.; Azam, A. Synthesis, characterization, antimicrobial activity and cytotoxicity of novel 2-(quinolin-8-yloxy) acetohydrazones and their cyclized products (1,2,3-thiadiazole and 1,2,3-selenadiazole derivatives). *Eur. J. Med. Chem.* **2010**, *45*, 6127-6134.
14. Revanasiddappa, H.D.; Kiran Kumar, T.N. A novel method for the spectrophotometric determination of thallium using methiomeprazine hydrochloride. *Turk. J. Chem.* **2005**, *29*, 265-272.

15. Ghorbanloo, M.; Jafari, S.; Bikas, R.; Krawczyk, M.S.; Lis, T. Dioxidovanadium(V) complexes containing thiazol-hydrazone NNN-donor ligands and their catalytic activity in the oxidation of olefins. *Inorg. Chim. Acta* **2017**, *455*, 15-24.
16. Nishihara, H. Multi-mode molecular switching properties and functions of azo-conjugated metal complexes. *Bull. Chem. Soc. Jpn.* **2004**, *77*, 407-428.
17. Ispir, E. The synthesis, characterization, electrochemical character, catalytic and antimicrobial activity of novel, azo-containing Schiff bases and their metal complexes. *Dyes Pigm.* **2009**, *82*, 13-19.
18. Sabet, R.A.; Khoshshima, H. Real-time holographic investigation of azo dye diffusion in a nematic liquid crystal host. *Dyes Pigm.* **2010**, *87*, 95-99.
19. Emam, S.M.; Abouel-Enein, S.A.; El-Saied, F.A.; Alshater, S.Y. Synthesis and characterization of some bi, tri and tetravalent transition metal complexes of N'-(furan-2-yl-methylene)-2-(p-tolylamino) acetohydrazide HL 1 and N'-(thiophen-2-yl-methylene)-2-(p-tolylamino)acetohydrazide HL 2. *Spectrochim. Acta Part A Mol. Biomol. Spectrosc.* **2012**, *92*, 96-104.
20. Liu, J.N.; Wu, B.W.; Zhang, B.; Liu, Y. Synthesis and characterization of metal complexes of Cu(II), Ni(II), Zn(II), Co(II), Mn(II) and Cd(II) with tetradentate schiff bases. *Turk. J. Chem.* **2006**, *30*, 41-48.
21. Svehla, G. *Vogel's Textbook of Macro and Semi Micro Quantitative Inorganic Analysis*. 5th ed., Longman: New York: **1979**; p 617.
22. Lewis, L.; Wilkins, R.G. *Modern Coordination Chemistry*. Interscience: New York; **1960**.
23. Collee, J.G.; Mackie, T.J.; McCartney, J.E. *Mackie and McCartney Practical Medical Microbiology*. 14th ed., Churchill Livingstone: New York; **1996**; p 978.
24. Gup, R.; Kirkan, B. Synthesis and spectroscopic studies of copper(II) and nickel(II) complexes containing hydrazonic ligands and heterocyclic coligand. *Spectrochim. Acta Part A Mol. Biomol. Spectrosc.* **2005**, *62*, 1188-1195.
25. Maurya, M.R.; Khurana, S.; Schulzke, C.; Rehder, D. Dioxo- and oxovanadium(V) complexes of biomimetic hydrazone ONO donor ligands: Synthesis, characterisation, and reactivity. *Eur. J. Inorg. Chem.* **2001**, *3*, 779-788.
26. Bessy Raj, B.N.; Prathapachandra Kurup, M.R.; Suresh, E. Synthesis, spectral characterization and crystal structure of N-2-hydroxy-4-methoxybenzaldehyde-N'-4-nitrobenzoyl hydrazone and its square planar Cu(II) complex. *Spectrochim. Acta Part A Mol. Biomol. Spectrosc.* **2008**, *71*, 1253-1260.
27. Bayoumi, H.A.; Alaghaz, A.-N.M.A.; Aljahdali, M.S. Cu(II), Ni(II), Co(II) and Cr(III) complexes with N2O2-chelating Schiff's base ligand incorporating azo and sulfonamide moieties: Spectroscopic, electrochemical behavior and thermal decomposition studies. *Int. J. Electrochem. Sci.* **2013**, *8*, 9399-9413.
28. Kurtoğlu, M.; Ispir, E.; Kurtoğlu, N.; Serin, S. Novel vic-dioximes: Synthesis, complexation with transition metal ions, spectral studies and biological activity. *Dyes Pigm.* **2008**, *77*, 75-80.
29. Oon Han, H.; Kim, S.H.; Kim, K.H.; Hur, G.C.; Joo Yim, H.; Chung, H.K.; Ho Woo, S.; Dong Koo, K.; Lee, C.S.; Sung Koh, J.; Kim, G.T. Design and synthesis of oxime ethers of α -acyl- β -phenylpropanoic acids as PPAR dual agonists. *Bioorg. Med. Chem. Lett.* **2007**, *17*, 937-941.
30. Geary, W.J. The use of conductivity measurements in organic solvents for the characterisation of coordination compounds. *Coord. Chem. Rev.* **1971**, *7*, 81-122.
31. Greenwood, N.N.; Straughan, B.P.; Wilson, A.E. Behaviour of tellurium(IV) chloride, bromide, and iodide in organic solvents and the structures of the species present. *J. Chem. Soc. A: Inorg. Phys. Theo.* **1968**, 2209-2212.

32. Xu, G.C.; Zhang, L.; Liu, L.; Liu, G.F.; Jia, D.Z. Syntheses, characterization and crystal structures of mixed-ligand Cu(II), Ni(II) and Mn(II) complexes of N-(1-phenyl-3-methyl-4-propenylidene-5-pyrazolone)-salicylidene hydrazide containing ethanol or pyridine as a co-ligand. *Polyhedron* **2008**, *27*, 12-24.
33. Samanta, B.; Chakraborty, J.; Shit, S.; Batten, S.R.; Jensen, P.; Masuda, J.D.; Mitre, S. Synthesis, characterisation and crystal structures of a few coordination complexes of nickel(II), cobalt(III) and zinc(II) with N'-(2-pyridyl)methylene]salicyloylhydrazone Schiff base. *Inorg. Chim. Acta* **2007**, *360*, 2471-2484.
34. Bhosale, J.D.; Shirolkar, A.R.; Pete, U.D.; Zade, C.M.; Mahajan, D.P.; Hadole, C.D.; Pawar, S.D.; Patil, U.D.; Dabur, R.; Bendre, R.S. Synthesis, characterization and biological activities of novel substituted formazans of 3,4-dimethyl-1Hpyrrole-2-carbohydrazide derivatives. *J. Pharm. Res.* **2013**, *7*, 582-587.
35. Singh, B.; Srivastava, P. Studies on 2,6-diacetylpyridine bis(2-furoylhydrazone) complexes of bivalent 3d-metal ions. *Transition Met. Chem.* **1987**, *12*, 475-477.
36. El-Wahab, Z.H.A.; Mashaly, M.M.; Salman, A.A.; El-Shetary, B.A.; Faheim, A.A. Co(II), Ce(III) and UO₂(VI) bis-salicylatothiosemicarbazide complexes: Binary and ternary complexes, thermal studies and antimicrobial activity. *Spectrochim. Acta Part A Mol. Biomol. Spectrosc.* **2004**, *60*, 2861-2873.
37. Chandra, S.; Gupta, L.K. Spectroscopic studies on Co(II), Ni(II) and Cu(II) complexes with a new macrocyclic ligand: 2,9-dipropyl-3,10-dimethyl-1,4,8,11-tetraaza-5,7:12,14-dibenzocyclotetradeca-1,3,8,10-tetraene. *Spectrochim. Acta Part A Mol. Biomol. Spectrosc.* **2005**, *61*, 1181-1188.
38. Nakamoto, K. *Infrared and Raman Spectra of Inorganic and Coordination Compounds Part B: Applications in Coordination, Organometallic, and Bioinorganic Chemistry*. 6th ed., John Wiley and Sons: New York; **2009**.
39. Gupta, L.K.; Bansal, U.; Chandra, S. Spectroscopic and physicochemical studies on nickel(II) complexes of isatin-3,2'-quinolyldiazones and their adducts. *Spectrochim. Acta Part A Mol. Biomol. Spectrosc.* **2007**, *66*, 972-975.
40. El-Tabl, A.S.; Shakhdoifa, M.M.E.; Shakhdoifa, A.M.E. Metal complexes of N'-[2-hydroxy-5-(phenyldiazenyl)-benzylidene] isonicotinohydrazide. Synthesis, spectroscopic characterization and antimicrobial activity. *J. Serb. Chem. Soc.* **2013**, *78*, 39-55.
41. El-Dissouky, A.; Fahmy, A.; Amer, A. Complexing ability of some γ -lactone derivatives. Thermal, magnetic and spectral studies on cobalt(II), nickel(II) and copper(II) complexes and their base adducts. *Inorg. Chim. Acta* **1987**, *133*, 311-316.
42. Al-Hakimi, A.N.; Shakhdoifa, M.M.E.; El-Seidy, A.M.A.; El-Tabl, A.S. Synthesis, spectroscopic, and biological studies of chromium(III), manganese(II), iron(III), cobalt(II), nickel(II), copper(II), ruthenium(III), and zirconyl(II) complexes of N1,N2-bis(3-((3-hydroxynaphthalen-2-yl)methylene-amino)propyl) phthalamide. *J. Korean Chem. Soc.* **2011**, *55*, 418-429.
43. Fouda, M.F.R.; Abd-Elzaher, M.M.; Shakhdoifa, M.M.; El-Saied, F.A.; Ayad, M.I.; El Tabl, A.S.; Synthesis and characterization of a hydrazone ligand containing antipyrine and its transition metal complexes. *J. Coord. Chem.* **2008**, *61*, 1983-1996.
44. Rageh, N.M.; Mawgoud, A.M.A.; Mostafa, H.M. Electronic spectra, solvatochromic behaviour, and acidity constants of some new azocoumarin derivatives. *Chem. Pap.* **1999**, *53*, 107-113.
45. Lever, A.B.P. *Inorganic Electronic Spectroscopy*. Elsevier Science: Amsterdam; **1984**.
46. Anitha, C.; Sheela, C.D.; Tharmaraj, P.; Johnson Raja, S. Synthesis and characterization of VO(II), Co(II), Ni(II), Cu(II) and Zn(II) complexes of chromone based azo-linked Schiff base ligand. *Spectrochim. Acta Part A Mol. Biomol. Spectrosc.* **2012**, *98*, 35-42.

47. El-Tabl, A.S.; Shakhofa, M.M.E.; Labib, A.A.; Al-Hakimi, A.N. Antimicrobial activities of the metal complexes of N'-(5-(4-chlorophenyl)diazenyl)-2-hydroxybenzylidene)-2-hydroxybenzohydrazide. *Main Group Chem.* **2012**, 11, 311-327.
48. Parihari, R.K.; Patel, R.K.; Patel, R.N. Synthesis and characterization of metal complexes of manganese-, cobalt- and zinc(II) with Schiff base and some neutral ligand. *J. Indian Chem. Soc.* **2000**, 77, 339-340.
49. Tiliakos, M.; Cordopatis, P.; Terzis, A.; P. Raptopoulou, C.; Perlepes, S.P.; Manessi-Zoupa, E. Reactions of 3d-metal nitrates with N,N'-bis(2-pyridyl)urea (LH₂): Preparation, X-ray crystal structures and spectroscopic studies of the products trans-[M(II)(ONO₂)₂(LH₂)₂] (M = Mn, Fe, Co, Ni, Cu, Zn) and mer-[Co(III)(LH)₂](NO₃)·MeOH. *Polyhedron* **2001**, 20, 2203-2214.
50. Al-Hakimi, A.N.; El-Tabl, A.S.; Shakhofa, M.M.E. Coordination and biological behaviour of 2-(p-toluidino)-N'-(3-oxo-1,3-diphenylpropylidene)acetohydrazide and its metal complexes. *J. Chem. Res.* **2009**, 12, 770-774.
51. Graham, B.; Spiccia, L.; Skelton, B.W.; White, A.H.; Hockless, D.C.R. Imidazole derivatives of binuclear copper(II) and nickel(II) complexes incorporating bis(1,4,7-triazacyclononan-1-yl) ligands. *Inorg. Chim. Acta* **2005**, 358, 3974-3982.
52. Wang, C.C. Refinement of the crystal structure of aquabis(2,2'-bipyridine)-bis(terephthalato)dycopper(II), Cu₂(H₂O)(C₁₀H₈N₂)₂(C₈H₄O₄)₂. *Z. Kristallograph. New Cryst. Struct.* **2006**, 221, 385-387.
53. Franklin, T.J.; Snow, G.A. *Biochemistry of Antimicrobial Action*, 4th ed., Chapman and Hall: London; **1989**; p 216.